

# On the Systematic Bias in the Estimation of Black Hole Masses in Active Galactic Nuclei

WANG Jianguo<sup>1,2,3\*</sup> & Dong Xiaobo<sup>4,5</sup>

<sup>1</sup>National Astronomical Observatories/Yunnan Observatory, Chinese Academy of Sciences, Kunming 650011, China;

<sup>2</sup>Key Laboratory for the Structure and Evolution of Celestial Objects, Chinese Academy of Sciences, Kunming 650011, China;

<sup>3</sup>Graduate University of Chinese Academy of Sciences, Beijing 100049, China

<sup>4</sup>Key Laboratory for Research in Galaxies and Cosmology, University of Science and Technology of China (USTC), Hefei 230026, China

<sup>5</sup>Center for Astrophysics, USTC, Hefei 230026, China

Received Apr. 26, 2012; accepted 000

In this report, we find the  $M_{\text{BH}}$  estimated from the formalism of Wang et al. (2009)[1] are more consistent with those from the  $M_{\text{BH}}-\sigma_*$  relation than those from previous single-epoch mass estimators, using a large sample of AGNs. Furthermore, we examine the differences between the line widths of H $\beta$  and Mg II in detail by comparing their line profiles. The flux around the line core and that in the wing of both H $\beta$  and Mg II show an opposite variation tendency, which indicates the BLR is multi-componential. The contribution of the wing makes the FWHM deviate from  $\sigma_{\text{line}}$ , and thus bias the  $M_{\text{BH}}$  estimated from previous single-epoch mass estimators. Thus the correction on the formalism suggested by Wang et al. (2009)[1] is crucial to  $M_{\text{BH}}$  estimation.

**Quasars, Galactic nuclei, Masses, Statistical and correlative studies of properties**

PACS: 98.54.Aj, 98.62.Js, 98.62.Ck, 98.62.Ve

## 1 Introduction

Accretion onto super-massive black holes (SMBHs) is generally considered as the energy engine of active galactic nuclei (AGNs). The determination of the mass of SMBH ( $M_{\text{BH}}$ ) is crucial to the understanding of most physical processes associated with SMBH and the cosmological evolution of black holes. The  $M_{\text{BH}}$  of type I AGNs are usually measured using the virial theorem,  $M_{\text{BH}}=fR_{\text{BLR}}V^2/G$ , if the size of broad line region ( $R_{\text{BLR}}$ ) and the virial velocity ( $V$ ) of clouds in the BLR are known, where  $f$  is a factor of order unity depending on the geometry and kinematics of the BLR.  $R_{\text{BLR}}$  can be estimated using the reverberation mapping (RM) method[2], which monitors the variability of continuum and emission lines.  $V$  can be estimated from the widths of emission lines. Conversely,  $M_{\text{BH}}$  can also be estimated using the tight correlation between  $M_{\text{BH}}$  and the stellar velocity dispersion of the galactic bulge ( $M_{\text{BH}}-\sigma_*$  relation)[3,4,5]. However, both of these methods cannot be used for large samples of AGNs,

because the RM method is time-consuming and the measurements of  $\sigma_*$  are limited by the spectral and spatial resolution of telescopes.

For large samples of AGNs,  $M_{\text{BH}}$  can be estimated by combining  $R_{\text{BLR}}$ , which is estimated using the important relationship between  $R_{\text{BLR}}$  and the monochromatic continuum luminosity (R-L relation)[6,7,8], and the FWHM of emission lines. The single-epoch mass estimators have been studied for various broad lines, such as H $\beta$  [1,9], H $\alpha$  [10], Mg II  $\lambda$ 2800 [1,11,12] and C IV  $\lambda$ 1549[13]. If both H $\beta$  and Mg II FWHMs are good tracers of the virial velocity and can be used to estimate the  $M_{\text{BH}}$ , they should give the same  $M_{\text{BH}}$  values. Some researchers found they are consistent with each other [11,14,15,16], while others came to an opposite conclusion [1,17,18]. Wang et al. (2009) found that Mg II FWHM is systematically smaller than H $\beta$  FWHM, and that the relationships between H $\beta$  and Mg II FWHM and  $\sigma_{\text{line}}$ , which is the best virial velocity tracer measured on the variable part of the spectrum[19], deviate from the 1:1 relationship. The dependence of  $M_{\text{BH}}$  on FWHM should be  $M_{\text{BH}}\propto\text{FWHM}^\gamma$ , where  $\gamma$  is smaller than 2 for both H $\beta$  and

\*Corresponding author (email: wangjg@ynao.ac.cn)

Mg II. If this is the case, most previous single-epoch mass estimators ( $M_{\text{BH}} \propto \text{FWHM}^2$ ) would introduce systematic biases in  $M_{\text{BH}}$  estimations [1,20,21,22,23] and result in many artificial conclusions, as discussed by Rafiee and Hall (2011)[21] and Croom (2011)[22]. Thus, further testing the validity of the formalism of Wang et al. (2009)[1] is critical for eliminating such biases in  $M_{\text{BH}}$  estimations and many other related relationships in AGNs. The  $M_{\text{BH}}$  estimated from the H $\beta$  and Mg II formalisms of Wang et al. (2009) are more consistent with those from RM measurements than those from previous single-epoch mass estimators and are consistent with each other for a large sample culled from Sloan Digital Sky Survey (SDSS) Data Release 5 (DR5). However, one remaining issue is whether the new  $M_{\text{BH}}$  estimates are consistent with those derived from the  $M_{\text{BH}}-\sigma_*$  relation, which should be tested using a large sample.

Moreover, the reasons for the systematic deviations between H $\beta$  and Mg II FWHM and  $\sigma_{\text{line}}$  are unclear now. The profile of an emission line is determined by the structure and kinematics of the BLR, which are complex. It is possible that the broad lines in most AGNs are generated in multi-regions, including the gravitationally-bound BLR, outflows [24] and the surface of accretion disk (Wang et al. 2005 [25]; Wu et al. 2008 [26]). Different measurements of line width, such as  $\sigma_{\text{line}}$  and FWHM, would represent different information about the structure and/or kinematics of the BLR. Special attention must be noted when using in the estimation of  $M_{\text{BH}}$ . The study of the structure and kinematics of the BLR would be helpful to understand why FWHM deviates from  $\sigma_{\text{line}}$  and important for the  $M_{\text{BH}}$  estimation of AGNs. In this report, we examine whether there are systematic biases between the  $M_{\text{BH}}$  estimated from the single-epoch mass estimators and those from the  $M_{\text{BH}}-\sigma_*$  relation. We also compare the profiles of H $\beta$  and Mg II in order to understand their differences and why their FWHM deviates from  $\sigma_{\text{line}}$ .

## 2 The Bias in the $M_{\text{BH}}$ Estimates

We first verify the consistency between the  $M_{\text{BH}}$  estimated from the single-epoch mass estimators and those from the  $M_{\text{BH}}-\sigma_*$  relation (Gültekin et al. 2009)[27]. We select 8470 AGNs with  $z < 0.35$  from SDSS DR4. The spectrum is corrected for the Galactic extinction using the extinction map of Schlegel et al. (1998)[28] and the reddening curve of Fitzpatrick (1999)[29]. The fitting method is described in Dong et al. (2008)[30] and described below. In the wavelength range 4030-7500Å, we fit simultaneously the featureless continuum and the Fe II multiplets and other emission lines. Each of the [O III]  $\lambda\lambda$  4959,5007 doublets is modeled with two Gaussians, one for the line core and the other for the possible blue wing. The narrow components of H $\alpha$  and H $\beta$  are fitted with similar profile to the line core of [O III]  $\lambda$ 5007 and the broad components of them are fitted with 1-4 gaussians.  $M_{\text{BH}}$  can be estimated using the width of the line core of [O III]  $\lambda$ 5007 as substitute for  $\sigma_*$  [31]. Be-

cause H $\beta$  is weak for many objects, we estimate H $\beta$  FWHM from H $\alpha$  FWHM [10] and then estimate the  $M_{\text{BH}}$  using the single-epoch mass estimators. We find that the differences between the  $M_{\text{BH}}$  estimated from the single-epoch mass estimators and those from the  $M_{\text{BH}}-\sigma_*$  relation are correlated with H $\alpha$  FWHM (Figure 1), if the formalisms from Greene and Ho (2005; hereafter GH05) [10] or Vestergaard and Peterson (2006; hereafter VP06) [9] are used. The correlation would decrease largely, if the formalism of Wang et al. (2009)[1] is adopted. The relationship between the  $M_{\text{BH}}$  differences and FWHM(H $\alpha$ ) is somewhat linear in log-log space and can be expressed as  $\log \frac{M_{\text{BH}}}{M_{\text{sig}}} = k \log \frac{\text{FWHM}(\text{H}\alpha)}{\text{kms}^{-1}} + b$ . The (k,b) for the formalisms of GH05, VP06 and Wang et al. (2009) given by the regression method of Kelly (2007)[32] are  $(2.05 \pm 0.04, -7.51 \pm 0.13)$ ,  $(1.93 \pm 0.03, -6.73 \pm 0.09)$  and  $(0.86 \pm 0.03, -2.99 \pm 0.11)$ , respectively. All the intrinsic scatters of these relations are around 0.02 dex. This indicates that the  $M_{\text{BH}}$  estimated from the formalism of Wang et al. (2009)[1] are less biased than those from previous single-epoch mass estimators ( $M_{\text{BH}} \propto \text{FWHM}^2$ ). We attempt to estimate the  $M_{\text{BH}}$  using the  $M_{\text{BH}}-\sigma_*$  relation from other authors (Xiao et al. 2011 [33]) and find the  $M_{\text{BH}}$  estimated from the formalism of Wang et al. (2009)[1] are still less biased than those from previous single-epoch mass estimators.

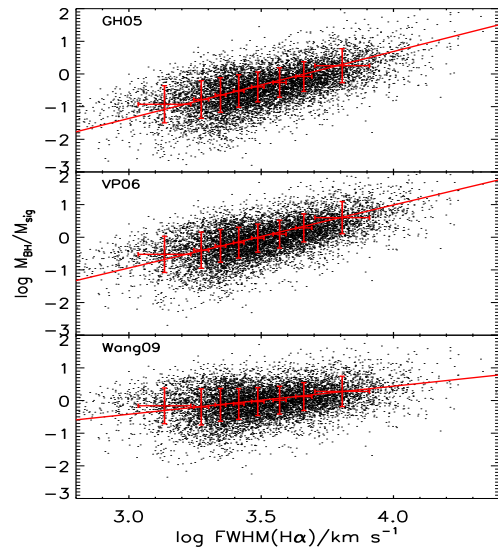


**Figure 1** Correlations between FWHM(H $\alpha$ ) and the differences of  $M_{\text{BH}}$  estimate from single-epoch mass estimators and those from  $M_{\text{BH}}-\sigma_*$  relation [27] for the sample from SDSS DR4. The crosses are the median values and standard deviations of the  $M_{\text{BH}}$  differences and FWHM in each bin of FWHM. The solid lines show the best-fit relations.

## 3 Profiles of H $\beta$ and Mg II

The comparison above shows that the method of Wang et al. (2009)[1] is capable of correcting the systematic biases in the

$M_{\text{BH}}$  estimations over a large redshift interval. This indicates indirectly that  $\text{H}\beta$  and  $\text{Mg II}$  FWHMs are deviating from  $\sigma_{\text{line}}$  systematically. The systematic deviation may be caused by the complex structure and kinematics of the BLR. We compare the profiles of  $\text{H}\beta$  and  $\text{Mg II}$  using the sample from Wang et al. (2009)[1], which was selected from SDSS DR5. The sample includes 495 AGNs with high signal-to-noise ratio ( $S/N > 20$ ) in both the  $\text{H}\beta$  (4600-5100 Å) and the  $\text{Mg II}$  (2700-2900 Å) regions, which makes it suitable for the comparison. The spectrum is corrected for the Galactic extinction using the extinction map of Schlegel et al. (1998)[28] and the reddening curve of Fitzpatrick (1999)[29]. The redshifts of these quasars are from Hewett and Wild (2010)[34], which were derived by cross-correlating observed spectra with a carefully constructed template. The dependence of emission line shift on luminosity and redshift are corrected and the systematic errors of redshifts are reduced to the level of 30 km/s, which are important to our investigation. We perform the continuum and emission-line fitting using an Interactive Data Language (IDL) code based on MPFIT [35], which performs  $\chi^2$ -minimization by the Levenberg-Marquardt technique.

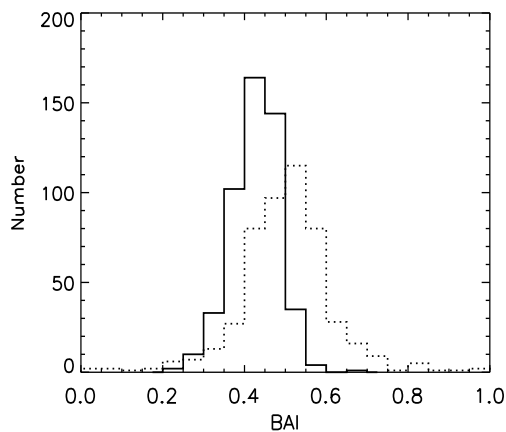


**Figure 2** BAI distributions of  $\text{H}\beta$  (solid line) and  $\text{Mg II}$  (dotted line).

The spectrum is fitted in two wavelength range:  $\text{H}\beta$  range (4200-5600 Å) and  $\text{Mg II}$  range (2200-3500 Å). For the  $\text{H}\beta$  range, the fitting method is similar to that described above. For the  $\text{Mg II}$  range, the method is described in Wang et al. (2009)[1]. The featureless continuum and  $\text{Fe II}$  multiplets were modeled simultaneously. The broad component of each of the  $\text{Mg II}\lambda\lambda$  2796,2803 doublets is modeled with a Gauss-Hermite series profile and the narrow component of each of the doublets is modeled by a Gaussian.

Usually, the shift and asymmetry of lines are studied separately, while they may be caused by the same process[24]. The blueshift and asymmetry index (BAI), which is defined as the flux ratio of the blue part to the total profile, measures their combined effects[24]. For  $\text{H}\beta$  and  $\text{Mg II}$ , the blue part is the part at wavelength short than 4862.68 and 2800.26 Å, respectively. The distributions of BAI are showed in Figure 2. The median value of the BAI distribution of  $\text{Mg II}$  is around

0.5, while that of  $\text{H}\beta$  is smaller than 0.5. Because both  $\text{H}\beta$  and  $\text{Mg II}$  show no evidence of shift (see Figure 3), the BAI is primarily caused by the line asymmetry. This indicates that  $\text{Mg II}$  profile is quite symmetrical in that there are more flux in the red part of  $\text{H}\beta$  than that in the blue part, which are consistent with the conclusion if the shift and asymmetry of lines are measured separately.

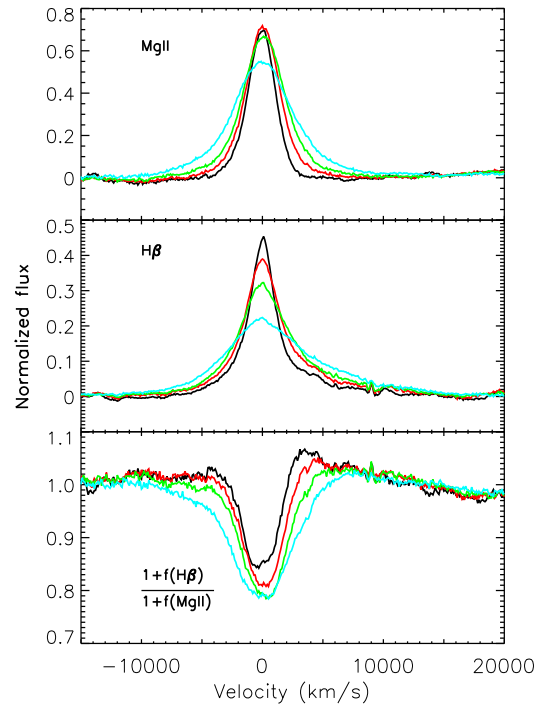


**Figure 3** Composite profiles of  $\text{H}\beta$  and  $\text{Mg II}$  of four sub-sample divided by their  $\text{H}\beta$  FWHM, as well as their difference in velocity space. First two panels are  $\text{H}\beta$  and  $\text{Mg II}$  profiles. All these flux are normalized at the emission-line-free window 3030 – 3090 Å and the continuum and  $\text{Fe II}$  multiplets were subtracted. The last panel shows the line ratios of  $\text{H}\beta$  and  $\text{Mg II}$ . Black:  $\text{FWHM}(\text{H}\beta) < 3000$  km/s; Red:  $3000$  km/s  $< \text{FWHM}(\text{H}\beta) < 4000$  km/s; Green:  $4000$  km/s  $< \text{FWHM}(\text{H}\beta) < 5500$  km/s; Cyan:  $\text{FWHM}(\text{H}\beta) > 5500$  km/s.

A direct comparison between the profiles of  $\text{H}\beta$  and  $\text{Mg II}$  is showed in Figure 3. The spectra are normalized at the emission-line-free window 3030 – 3090 Å and the featureless continuum and  $\text{Fe II}$  multiplets are subtracted. The sample is divided into four sub-samples according to  $\text{H}\beta$  FWHM. The composite  $\text{H}\beta$  and  $\text{Mg II}$  profiles of each sub-sample, as well as their line ratio, are showed in Figure 3. The peaks of both  $\text{H}\beta$  and  $\text{Mg II}$  do not show evident shift. The flux in the wings increases with the increase of FWHM, while the flux around the line core decreases with the increase of FWHM. The change of  $\text{H}\beta$  is more rapid than that of  $\text{Mg II}$ . This indicates that  $\text{H}\beta$  and  $\text{Mg II}$  are not cospatial in BLR and the BLR in AGNs is multi-componential. At least two emitting regions are needed: an intermediate line region (ILR) producing the line core and a very broad line region (VBLLR) producing the

line wings[36]. The emission in ILR makes larger contribution to the Mg II lines, while the emission in the VBLR makes larger contribution to the Balmer lines[36].

#### 4 Discussion

Different structures of the BLR have been proposed to explain the profiles of emission lines. These models includes: a rotating accretion disk, binary black holes, bipolar outflow and anisotropically illuminated spherical BLR (see Eracleous and Halpern 2003 and reference therein)[37], as well as the gravitationally-bound BLR+outflow model of Wang et al. (2011)[24]. The gravitationally-bound BLR+outflow model has succeeded in explaining the profiles of the high ionization C IV line[24], but is not suitable to explain the profile of low ionization H $\beta$  line. This is because H $\beta$  shows a systematically small BAI (<0.5) opposed to the expectation of the model (BAI>0.5). Eracleous and Halpern (2003) found the accretion disk emission could explain the double-peak profile and other spectroscopic properties of AGNs presenting the double-peaked Balmer lines, while other structures are unsatisfactory[37]. They attempted to explain the profiles of H $\beta$  and Mg II using the accretion disk emission, but the model predicts lower Mg II flux than the observed flux. One of the possible reasons is that the BLR is two-componential. The contribution of the ILR to Mg II is critical but is not included in their model.

As showed in Figure 3, the contribution of the VBLR to H $\beta$  and Mg II flux becomes more important with the increase of H $\beta$  FWHM. However, the contribution of the VBLR to  $\sigma_{line}$  may be small, because clouds in the VBLR might be optically thin to the ionization continuum[38]. The emission from the VBLR does not vary with the variability of continuum and contributes little to the variable part of the spectrum. This may be the reason of the systematic deviations between H $\beta$  and Mg II FWHM and  $\sigma_{line}$ . Moreover, the fraction of the contribution of the VBLR to Mg II is much smaller than that to H $\beta$ , which makes the Mg II FWHM systematically smaller than H $\beta$  FWHM. The contribution of the VBLR makes FWHM deviate from  $\sigma_{line}$  systematically and bias the  $M_{BH}$  estimation from previous single-epoch mass estimators ( $M_{BH} \propto FWHM^2$ ). When estimating the  $M_{BH}$  using FWHM as the tracer of the virial velocity, it is crucial to correct the biases by using the fitted index of the  $M_{BH} \propto FWHM^\gamma$  relation, rather than the assumed  $\gamma = 2$ , as suggested by Wang et al. (2009).

*We thank the anonymous referees for their helpful suggestions that improved the paper. We acknowledge useful comments and suggestions from Weimin Yuan and Chang You. This work was supported by Chinese NSF (grant Nos. 11073019, 10973034, 11033007, 11133006 and 11103071) and the National Basic Research Program of (973 Program) 2009CB824800.*

- 1 Wang J G, Dong X B, Wang T G, et al. Estimating Black Hole Masses in Active Galactic Nuclei Using the Mg II  $\lambda$ 2800 Emission Line. *Astrophys J*, 2009, 707: 1334–1346
- 2 Blandford R D, McKee C F. Reverberation mapping of the emission line regions of Seyfert galaxies and quasars. *Astrophys J*, 1982, 255: 419–439
- 3 Gebhardt K, Kormendy J, Ho L C, et al. Black Hole Mass Estimates from Reverberation Mapping and from Spatially Resolved Kinematics. *Astrophys J*, 2000, 543: L5–L8
- 4 Ferrarese L, Pogge R W, Peterson B M, et al. Supermassive Black Holes in Active Galactic Nuclei. I. The Consistency of Black Hole Masses in Quiescent and Active Galaxies. *Astrophys J*, 2001, 555: L79–L82
- 5 Onken C A, Peterson B M, Dietrich M, et al. Black Hole Masses in Three Seyfert Galaxies. *Astrophys J*, 2003, 585: 121–127
- 6 Kaspi S, Smith P S, Netzer H, et al. Reverberation Measurements for 17 Quasars and the Size-Mass-Luminosity Relations in Active Galactic Nuclei. *Astrophys J*, 2000, 533: 631–649
- 7 Bentz M C, Peterson B M, Pogge R W, et al. The Radius-Luminosity Relationship for Active Galactic Nuclei: The Effect of Host-Galaxy Starlight on Luminosity Measurements. *Astrophys J*, 2006, 644: 133–142
- 8 Bentz M C, Peterson B M, Netzer H, et al. The Radius-Luminosity Relationship for Active Galactic Nuclei: The Effect of Host-Galaxy Starlight on Luminosity Measurements. II. The Full Sample of Reverberation-Mapped AGNs. *Astrophys J*, 2009, 697: 160–181
- 9 Vestergaard M, Peterson B M. Determining Central Black Hole Masses in Distant Active Galaxies and Quasars. II. Improved Optical and UV Scaling Relationships. *Astrophys J*, 2006, 641: 689–709
- 10 Greene J E, Ho L C. Estimating Black Hole Masses in Active Galaxies Using the H $\alpha$  Emission Line. *Astrophys J*, 2005, 630: 122–129
- 11 McLure R J, Jarvis M J. Measuring the black hole masses of high-redshift quasars. *Mon Not Roy Astron Soc*, 2002, 337: 109–116
- 12 Kong M Z, Wu X B, Wang R, et al. Estimating Black Hole Masses of AGNs using Ultraviolet Emission Line Properties. *China J. Astron Astrophys*, 2006, 6: 396–410
- 13 Vestergaard M. Determining Central Black Hole Masses in Distant Active Galaxies. *Astrophys J*, 2002, 571: 733–752
- 14 Salvander I S, Shields G A, Gebhardt K, et al. The Black Hole Mass-Galaxy Bulge Relationship for QSOs in the Sloan Digital Sky Survey Data Release 3. *Astrophys J*, 2007, 662: 131–144
- 15 Hu C, Wang J M, Ho L C, et al. A Systematic Analysis of Fe II Emission in Quasars: Evidence for Inflow to the Central Black Hole. *Astrophys J*, 2008, 687: 78–96
- 16 Shen Y, Richards G T, Strauss M A, et al. A Catalog of Quasar Properties from Sloan Digital Sky Survey Data Release 7. *Astrophys J Suppl Ser*, 2011, 194: 45
- 17 Corbett E A, Croom S M, Boyle B J, et al. Emission linewidths and QSO black hole mass estimates from the 2dF QSO Redshift Survey. *Mon Not Roy Astron Soc*, 2003, 343: 705–718
- 18 Dietrich M, Hamann F. Implications of Quasar Black Hole Masses at High Redshifts. *Astrophys J*, 2004, 611: 761–769
- 19 Peterson B M, Ferrarese L, Gilbert K M, et al. Central Masses and Broad-Line Region Sizes of Active Galactic Nuclei. II. A Homogeneous Analysis of a Large Reverberation-Mapping Database. *Astrophys J*, 2004, 613: 682–699
- 20 Rafiee A, Hall P B. Supermassive Black Hole Mass Estimates Using Sloan Digital Sky Survey Quasar Spectra at  $0.7 < z < 2$ . *Astrophys J Suppl Ser*, 2011, 194: 42
- 21 Rafiee A, Hall P B. Biases in the quasar mass-luminosity plane. *Mon*

- Not Roy Astron Soc, 2011, 415: 2932–2941
- 22 Croom S M. Do Quasar Broad-line Velocity Widths Add Any Information to Virial Black Hole Mass Estimates? *Astrophys J*, 2011, 736: 161
- 23 Peterson B M. Masses of Black Holes in Active Galactic Nuclei: Implications for NLS1s. arXiv:1109.4181
- 24 Wang H Y, Wang T G, Zhou H Y, et al. Coexistence of Gravitationally-bound and Radiation-driven CIV Emission Line Regions in Active Galactic Nuclei. *Astrophys J*, 2011, 738: 85
- 25 Wang T G, Dong X B, Zhang X G, et al. Two Extreme Double-peaked Line Emitters in the Sloan Digital Sky Survey. *Astrophys J*, 2005, 625: L35–L38
- 26 Wu S M, Wang T G, Dong X B. Broad reprocessed Balmer emission from warped accretion discs. *Mon Not Roy Astron Soc*, 2008, 389: 213–222
- 27 Gültekin K, Richstone D O, Gebhardt K, et al. The  $M-\sigma$  and  $M-L$  Relations in Galactic Bulges, and Determinations of Their Intrinsic Scatter. *Astrophys J*, 2009, 698: 198–221
- 28 Schlegel D J, Finkbeiner D P, Davis M. Maps of Dust Infrared Emission for Use in Estimation of Reddening and Cosmic Microwave Background Radiation Foregrounds. *Astrophys J*, 1998, 500: 525
- 29 Fitzpatrick E L. Correcting for the Effects of Interstellar Extinction. *Publ Astron Soc Pac*, 1999, 111: 63–75
- 30 Dong X B, Wang T G, Wang J G, et al. Broad-line Balmer decrements in blue active galactic nuclei. *Mon Not Roy Astron Soc*, 2008, 383: 581–592
- 31 Komossa S, Xu D. Narrow-Line Seyfert 1 Galaxies and the  $M_{\text{BH}}-\sigma$  Relation. *Astrophys J*, 2007, 667: L33–L36
- 32 Kelly B C. Some Aspects of Measurement Error in Linear Regression of Astronomical Data. *Astrophys J*, 2007, 665: 1489–1506
- 33 Xiao T, Barth A J, Greene J E, et al. Exploring the Low-mass End of the  $M_{\text{BH}}-\sigma_*$  Relation with Active Galaxies. *Astrophys J*, 2011, 739: 28
- 34 Hewett P C, Wild V. Improved redshifts for SDSS quasar spectra. *Mon Not Roy Astron Soc*, 2010, 405: 2302–2316
- 35 Markwardt C B. Non-linear Least-squares Fitting in IDL with MPFIT. In: David A, Bohlender D D, Patrick D, eds. Proceedings of the conference held 2-5 November 2008 at Hotel Loews Le Concorde, Québec City, QC, Canada, 2009, 411: 251–254
- 36 Popović L Č, Mediavilla E, Bon E, et al. Contribution of the disk emission to the broad emission lines in AGNs: Two-component model. *Astron & Astrophys*, 2004, 423: 909–918
- 37 Eracleous M, Halpern J P. Completion of a Survey and Detailed Study of Double-peaked Emission Lines in Radio-loud Active Galactic Nuclei. *Astrophys J*, 2003, 599: 886–908
- 38 Ferland G J, Korista K T, Peterson B M. Optically thin thermal emission as the origin of the big bump in the spectra of active galactic nuclei. *Astrophys J*, 1990, 363: L21–L25